N87-25895

HIGH TEMPERATURE ELECTROLYZER/FUEL CELL POWER CYCLE: PRELIMINARY DESIGN CONSIDERATIONS

Jeffrey H. Morehouse
Associate Professor
Mechanical Engineering Department
University of South Carolina
Columbia, SC 29208

A model of a high temperature electrolyzer/fuel cell, hydrogen/oxygen, thermally regenerative power cycle is developed and used to simulate system performance for varying system parameters. Initial estimates of system efficiency, weight, and volume are provided for a one KWe module assuming specific electrolyzer and fuel cell characteristics, both current and future. Specific interest is placed on examining the system responses to changes in device voltage versus current density operating curves, and the associated optimum operating ranges.

The performance of a solar-powered, space-based system in low earth orbit is examined in terms of the light-dark periods requiring storage. The storage design tradeoffs between thermal energy, electrical energy, and hydrogen/oxygen mass storage are examined. The current technology module is based on the 1000°C solid oxide electrolyzer cell and the alkaline fuel cell. The "Future Technology" system examines benefits involved with developing a 1800K electrolyzer operating with an advanced fuel cell.

NASA Colleague: Thomas L. Davies EP5 X3133

TABLE OF CONTENTS

INTRODUCTION

The renewed interest in space-based activities, both NASA-related and "Star Wars" related, has led to the examination of numerous types of power systems which might be appropriate for space applications [Refs. 1,2]. The energy source for these power systems is envisioned as being either nuclear or solar energy. Both sources supply thermally-driven dynamic systems, with solar able to use photovoltaic systems to directly produce electricity.

The possibility of thermally-driving a fuel cell power system is attractive from several engineering aspects, as it combines some of the better features of both photovoltaic (PV) and dynamic systems. Like the PV system, a fuel cell power cycle can produce electricity without the rotating motor-generator mechanical components. Moreover, the fuel cell power cycle is capable of higher efficiencies than PV systems; much closer to the higher dynamic system thermal efficiencies. As the fuel cell cycle is thermally-driven, it can operate during a complete light-dark orbit using stored thermal energy, similar to the dynamic system operating concept. A hydrogen-oxygen fuel cell is proposed because of high efficiency and because using water as the working fluid with space missions has several inherent advantages, including crew compatibility (non-toxic, life supporting) and possible use as a reaction fuel.

HIGH TEMPERATURE ELECTROLYZER/FUEL CELL CYCLE CONCEPT

The development of the basic relations for the high temperature electrolysis/fuel cell system is based on the water dissociation energy reaction:

$$H_2 + 1/2O_2 \rightleftharpoons H_2O \qquad (1)$$

The dissociation energy or energy of reaction (ΔH_f) is a mild function of reaction temperature, as seen in Figure 1. For an isothermal reaction, this ΔH_f can be thought of as "ideally" consisting of two parts or types of energy input (or output, depending on the direction of reaction):

$$\Delta H_f = \Delta G_f + T^\circ \Delta S_f \qquad (2)$$

where,

ΔG_f is the Gibb's free energy, the available work (ideal work)

$T^\circ \Delta S_f$ is the isothermal heat transfer (ideal heat transfer)

As is seen in Figure 1, the ideal heat and work in the water reaction are strong functions of the reaction temperature. This property of the water reaction is what permits operation of a thermally regenerative fuel cell cycle. At high temperatures, a small amount of work is available from the hydrogen-oxygen association reaction.

The High Temperature Electrolyzer/Fuel Cell (HTE) system consists of an electrolyzer operating at high temperature, T_H, a regenerative heat exchanger, and a fuel cell operating at low temperature, T_C. The electrolyzer is run

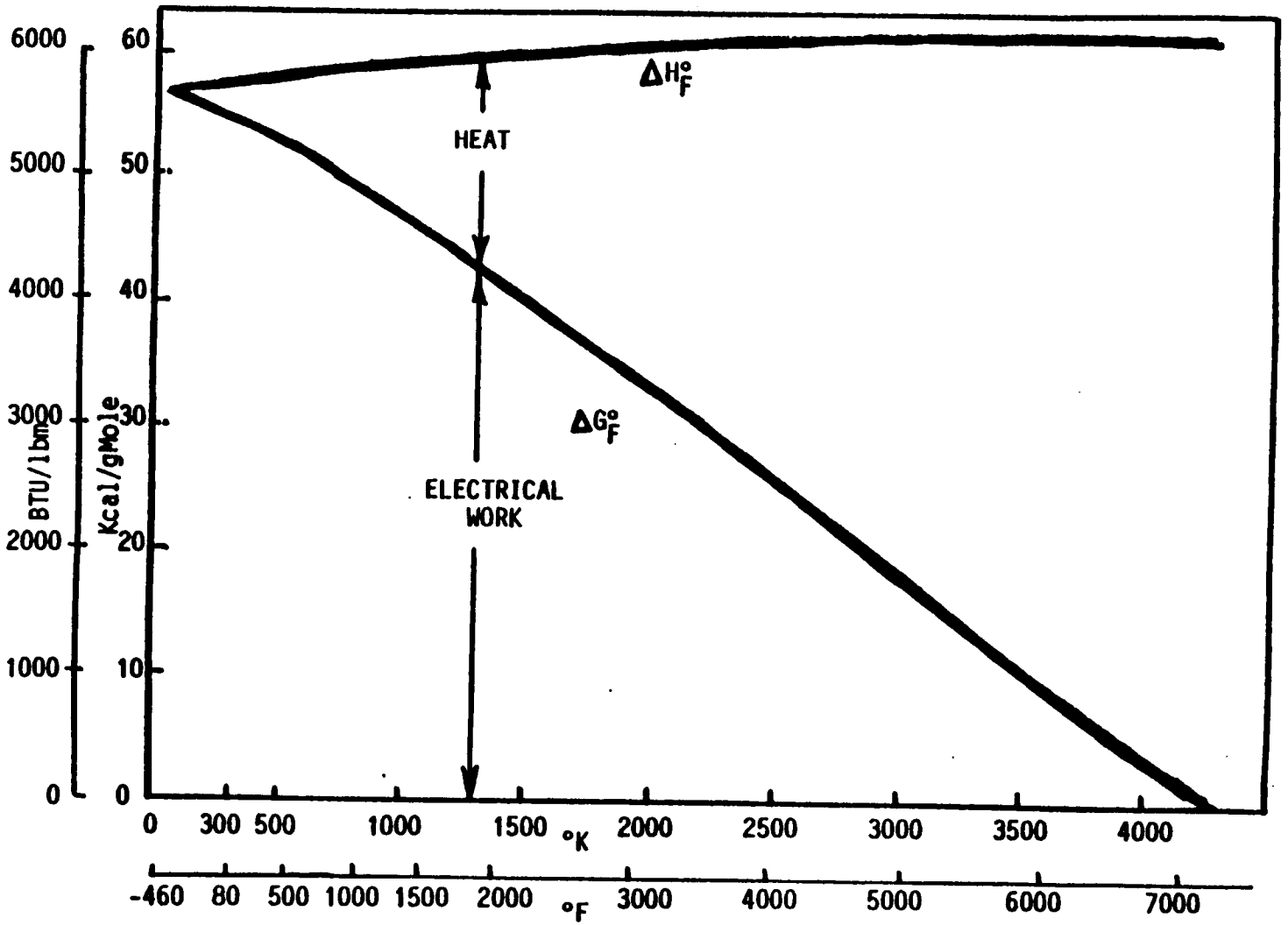

Figure 1. DISSOCIATION ENERGY (ΔH_F°) AND GIBB'S FREE (ΔG_F°) ENERGY AS A FUNCTION OF TEMPERATURE FOR WATER

from the electrical output of the fuel cell, plus a high temperature heat input. The cycle net work output consists of the fuel cell's electrical work which exceeds the electrolyzer requirements; this net work is graphically illustrated as the difference between ΔG's at two temperatures on Figure 1. The basic HTE heat engine schematic is shown in Figure 2 with heat input at high temperature where water is electrolyzed into hydrogen and oxygen, a regenerative heat exchange between the water and hydrogen-oxygen, and a fuel cell producing electrical energy while rejecting heat.

HTE CYCLE INVESTIGATIONS

The HTE power cycle was described thermodynamically as early as 1959 [Refs. 3,4,5]. These early analyses dealt with the cycle conceptually and defined ideal cycle efficiency and its relation to Carnot efficiency. While work on high temperature electrolyzers has continued to be of interest, the primary thrust has been directed towards producing hydrogen as a fuel [Refs. 6,7]. However, the energy situation in the 70's did stimulate interest in solar energy and thus, in thermally regenerative electrochemical systems [Ref. 8]. Those studies which did examine HTE cycles concluded that these cycles were not of practical interest since no high temperature electrolyzer existed [Refs. 8,9]. More recently, it has been suggested that the high temperature electrolyzers under development may be appropriate for the HTE cycle [Refs. 10, 11].

The present approach to development of high temperature electrolyzers and fuel cells involves the use of a solid oxide electrolyte (SOE). In the USA, the Department of Energy sponsors much of the solid oxide fuel cell development work [Refs. 12-15], while the German emphasis is on a SOE nicknamed "Hot

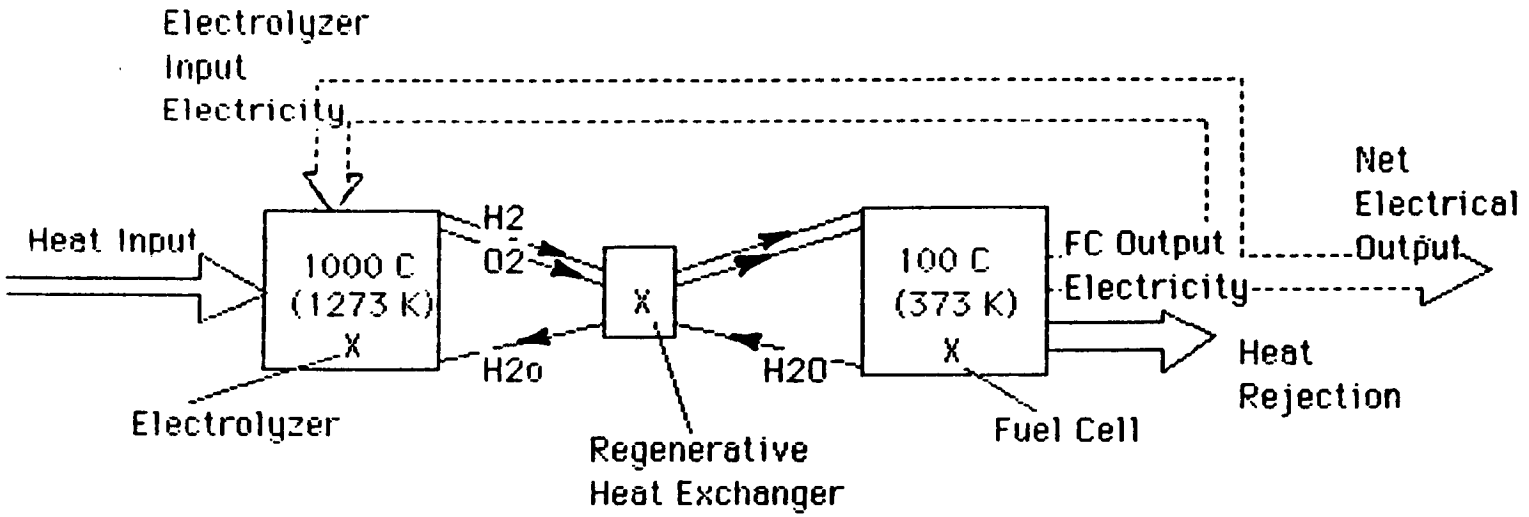

Figure 2. SCHEMATIC OF THERMALLY-DRIVEN REGENERATIVE FUEL CELL HEAT ENGINE

Elly" [Refs. 16,17]. The solid oxide cell being developed has a 30-micron thick solid electrolyte consisting of a Yttria-stablized Zirconia. Currently, the cell stacks are being tested in the 1300°K range. Single cells have been tested for hundreds of hours without degradation and with near-theoretical open-circuit voltage.

DESCRIPTION OF WORK

The objective of this work is to examine the high temperature electrolyzer/fuel cell power cycle for preliminary design and sizing considerations. The examination includes looking at both individual devices and the overall system characteristics and performance.

Scope of Work

A model of the HTE cycle is developed and used to simulate system performance for varying system parameters. Initial estimates of system efficiency, weight, and volume are provided for a 1 KWe module assuming specific electrolyzer and fuel cell characteristics, both current and future. Specific interest is placed on examining the system responses to changes in device voltage versus current density operating curves, and the associated optimum operating ranges. "Current Technology" is based on the 1000°C solid oxide electrolyzer cell and the alkaline fuel cell. The "Future Technology" system examines benefits involved with developing a 1800K electrolyzer operating with an advanced fuel cell.

The performance of a solar-powered, space-based system in low earth orbit is examined in terms of the light-dark periods requiring storage. The storage design tradeoffs between thermal energy, electrical energy, and hydrogen/oxygen mass storage are examined.

A computer program was developed to simulate the HTE cycle. The basic equations and definitions used with the cycle and each device have been previously described [Refs. 10, 11]. Figure 3 illustrates the logic used in the program to simulate the HTE cycle.

Figure 3.

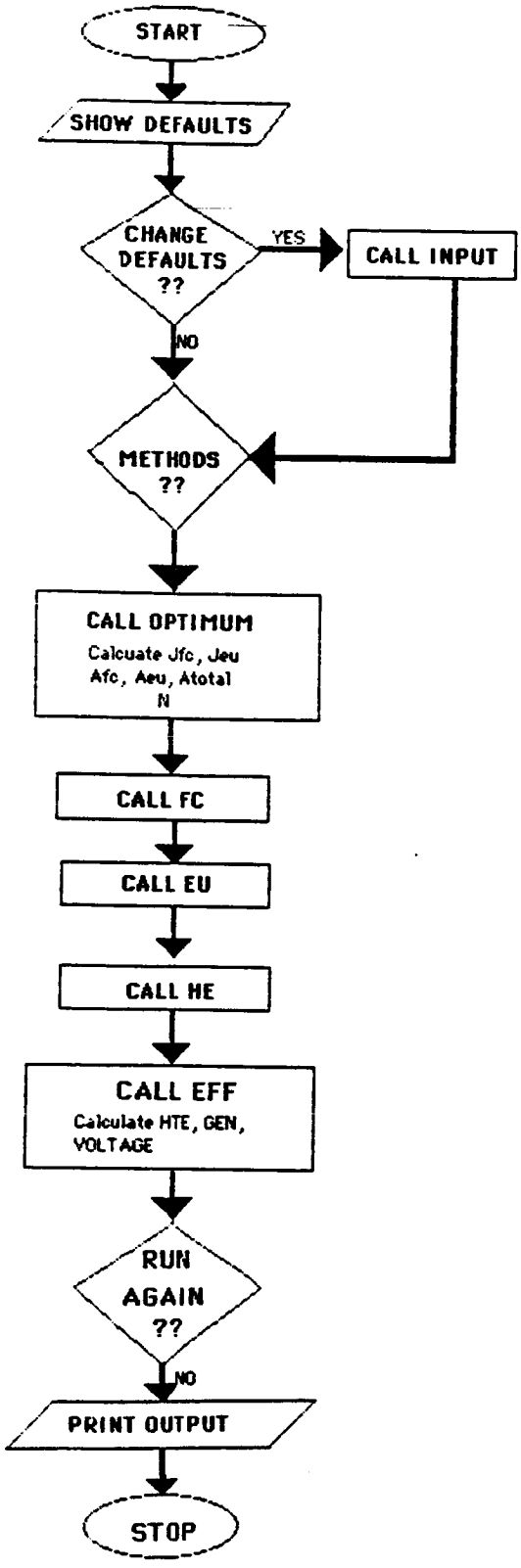
START
SHOW DEFAULTS
CHANGE DEFAULTS ??
YES
CALL INPUT
NO
METHODS ??
CALL OPTIMUM
Calcuate Jfc, Jeu
Afc, Aeu, Atotal
N
CALL FC
CALL EU
CALL HE
CALL EFF
Calculate HTE, GEN, VOLTAGE
RUN AGAIN ??
NO
PRINT OUTPUT
STOP

Current and Future Technology

The description of the fuel cell and electrolyzer devices was in terms of performance and physical measurements. For the computer model, the device cell performance was indicated by the polarization curve (voltage versus current density), plus the cell current efficiency. The physical measurements (volume, mass) of the devices were examined on a unit cell-area basis.

1. Polarization Curves

The polarization curves of cell voltage versus current density are presented in Figure 4 for both the current and future technology fuel cells and electrolyzers. The current technology fuel cell (alkaline) polarization curve was taken from an alkaline cell developed for NASA [Ref. 18]. The future fuel cell is a projection of what an acid (SPE-type) cell would exhibit with greatly reduced electrode-electrolyte resistance and concentration effects. These polarization relations (linearized) are (with V in volts, J in ma/cm^2):

$$\text{Future FC:} \quad V = 1.16 - 0.000667J$$

$$\text{Current FC:} \quad V = 1.14 - 0.0045J \quad (0 < J \leq 20)$$

$$V = 1.05 - 0.00275J \quad (20 < J \leq 40)$$

$$V = 0.995 - 0.0006J \quad (40 < J)$$

The current technology electrolyzer cell polarization curve was taken from data on the solid oxide electrolyte (SOE) under development [Ref. 19]. The projected technology 1500K and 1800K SOE cell curves are based on similar internal resistances and equivalent approach to ideal open circuit voltage.

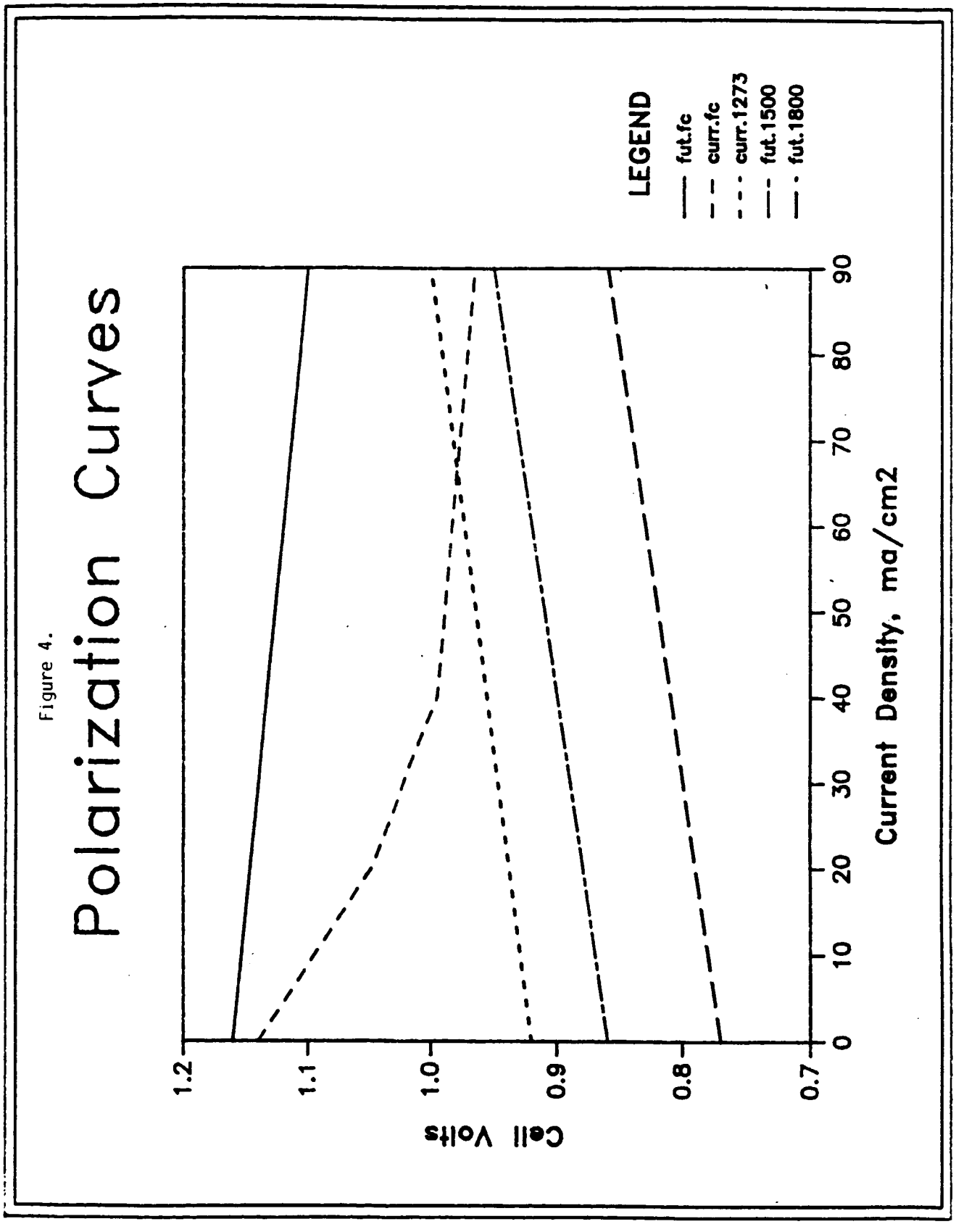
Polarization Curves
LEGEND
fut.fc
curr.fc
curr.1273
fut.1500
fut.1800
Cell Volts
1.2
1.1
1.0
0.9
0.8
0.7
0
10
20
30
40
50
60
70
80
90
Current Density, ma/cm2

Figure 4.

The equations for these electrolyzer cells are:

Current SOE (1273K): $V = 0.92 + 0.000889J$

Future SOE (1500K): $V = 0.86 + 0.001J$

Future SOE (1800K): $V = 0.77 + 0.001J$

2. Physical Measurements

The values for the current and future technology fuel cell and electrolyzer volume and mass per unit cell-area presented in Table 1. The values for the current technology fuel cell and electrolyzer are taken from developmental work on the NASA Space Station project [Ref. 20]. The future technology values are for SPE-type fuel cells and SOE electrolyzer cells.

TABLE 1 . MASS AND VOLUME VALUES

CURRENT TECHNOLOGY	MASS (kg/m2 of cell area)	VOLUME (m3/m2 of cell area)
o Fuel Cell		
-Alkaline	8.1	0.014
-Acid	2	0.01
o Electrolyzer		
-Alkaline	16.6	0.02
-Solid Oxide (1000 C)	26.2	0.013
FUTURE TECHNOLOGY		
o Fuel Cell	2	0.01
o Electrolyzer		
-Solid Oxide (1500 K)	6.5	0.01
-Solid Oxide (1800 K)	6.5	0.01

STORAGE OPTIONS

In solar powered systems, energy storage is necessary for operation during sunless periods. For a solar system in a 270 nautical mile high equatorial orbit, the 95 minute orbital period would consist of 59 minutes of sun (TS) and 36 minutes of dark (TD). Thus, the HTE cycle has to collect enough energy during the sun period both to operate the system and to charge the storage system.

Three storage options are examined for their effect on overall system efficiency and design:

1) Thermal storage - collected high temperature thermal energy is stored before it is input to the HTE cycle;
2) Chemical storage - H2 and O2 are stored within the HTE cycle; and
3) Electrical storage - electrical energy output from the HTE cycle is stored prior to delivery.

These three options are shown schematically as located in the overall system in Figure 5.

For purposes of comparing these three storage options, the following assumptions are made concerning the HTE cycle and overall system conditions:

- Output - 25 kWe continuously delivered to the load during sun and dark periods.
- Input - 1354 w/m^2 solar flux with a 70 percent collection efficiency provides the collected thermal energy input.
- HTE cycle - Electrolyzer at 1273K and the fuel cell at 373K, with actual cycle efficiency of 33 percent (= 1/2 of ideal efficiency).

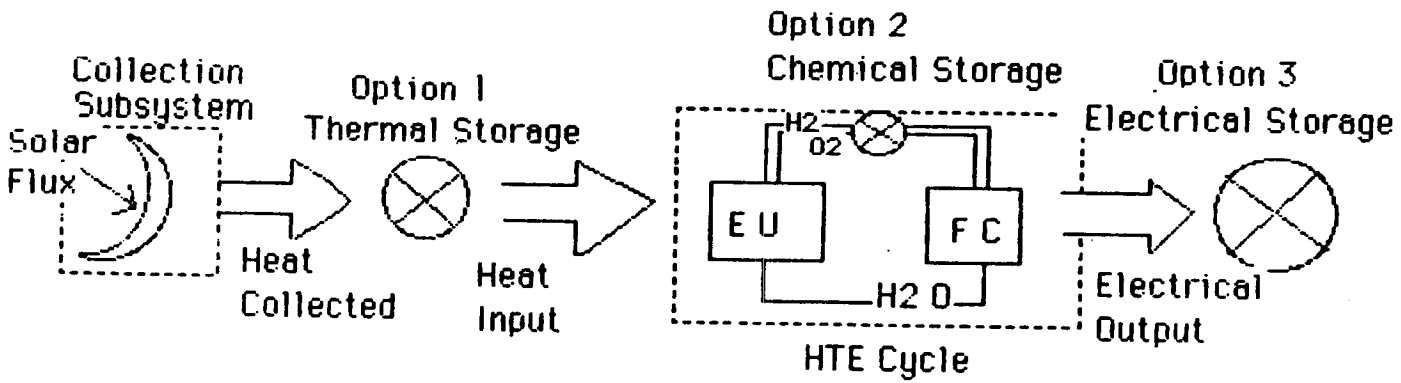
Collection
Subsystem
Solar
Flux
Heat
Collected
Option 1
Thermal Storage
Heat
Input
Option 2
Chemical Storage
H2
02
E U
F C
H2 O
HTE Cycle
Option 3
Electrical Storage
Electrical
Output

Figure 5.

System Efficiencies

The overall system efficiency is based on the ratio of the electrical energy delivered to the solar energy input:

$$\eta_{os} = \frac{\text{Electrical Energy Delivered}}{\text{Solar Energy Intercepted}}$$

The overall system is assumed to consist of three subsystems and their associated efficiencies: collection, HTE cycle, and storage subsystems. The overall system efficiency can be expressed in terms of the three subsystem efficiencies as:

$$\eta_{os} = \eta_{coll} \cdot \eta_{stor} \cdot \eta_{cyc}$$

Since for all storage options the collection subsystem is unchanged, it is convenient to write

$$\eta_{sys} = \eta_{stor} \cdot \eta_{cyc} = \frac{\text{Electrical Energy Delivered}}{\text{Thermal Energy Collected}}$$

where, $\eta_{stor} = \frac{\text{Energy From Storage}}{\text{Energy Input to Storage}}$

$$\eta_{cyc} = \frac{\text{Electrical Output}}{\text{Thermal Input}}$$

The power delivered (Pdel) is required both during sun and dark (TS+TD), while the solar energy collected must be done during sun (TS). So,

$$\eta_{sys} = \frac{\text{Energy Delivered}}{\text{Energy Collected}} = \frac{Pdel \cdot (TS + TD)}{Pcol \cdot TS}$$

where Pcol is the rate of energy collection.

It is also seen that the thermal energy collected can be thought of as

being used in two ways:

$$\text{Energy Collected} = \text{Energy used directly} + \text{Energy stored}$$

The energy used directly will provide power during the sun period and will only involve the HTE cycle:

$$P_{del} \cdot TS = \eta_{cyc} \cdot (\text{Energy Used Directly}).$$

The energy stored will provide power during the dark period and will involve both storage and HTE cycle subsystems:

$$P_{del} \cdot TD = \eta_{stor}\eta_{cyc} \cdot (\text{Energy Stored})$$

So, substituting yields:

$$P_{col} \cdot TS = \frac{P_{del} \cdot TS}{\eta_{cyc}} + \frac{P_{del} \cdot TD}{\eta_{stor}\eta_{cyc}}$$

and $$\frac{P_{col}}{P_{del}} = \frac{1}{TS}\left(\frac{TS}{\eta_{cyc}} + \frac{TD}{\eta_{stor}\eta_{cyc}}\right)$$

which can be substituted back into the η_{sys} equation to give the general expression to be used for the storage-system efficiency relationship:

$$\eta_{sys} = \eta_{\frac{cyc \cdot (TS+TD)}{TS + \frac{TD}{\eta_{stor}}}} \qquad (3)$$

In the sections below, each of the three storage options is examined for efficiency and subsystem sizing effects.

1. Thermal Storage

The thermal storage option consists of placing the thermal storage between the collection and HTE cycle subsystems, as shown in Figure 6. During sun periods, the HTE cycle is driven directly from the energy collected to produce 25 kWe. During dark periods, the HTE cycle is driven from storage to produce 25 kWe. Thus, the HTE cycle should be sized to produce 25 kWe.

The system efficiency from Eq. 3, with thermal storage being 90 percent efficient, is 31.7 percent. This gives an overall system efficiency of 22.2 percent with a required collector area of 133.9 m^2.

While operating at 1300K, the thermal storage unit must be sized to accept 50.5 kWHR of thermal energy input at a rate of 51.4 kW. The unit must also discharge 45.5 kWHR of thermal energy at 75.8 kW.

2. Electrical Storage

The electrical storage configuration is shown in Figure 7, with the storage located between the HTE cycle and the electrical load. The HTE cycle operates only during the sun period, and must supply both the load and the energy to charge the electrical storage during this period. The energy which must be delivered by the HTE cycle is given by:

$$\text{HTE Energy Delivered} = \text{Pdel} \cdot \text{TS} + \frac{\text{Pdel} \cdot \text{TD}}{\eta_{\text{stor}}}$$

And since this energy must be delivered during sun, TS, then the HTE cycle must be sized to produce power at:

$$\text{HTE Power} = \frac{\text{HTE Energy Delivered}}{\text{TS}} = \text{Pdel}\left(1 + \frac{\text{TD}}{\text{TS} \cdot \eta_{\text{stor}}}\right)$$

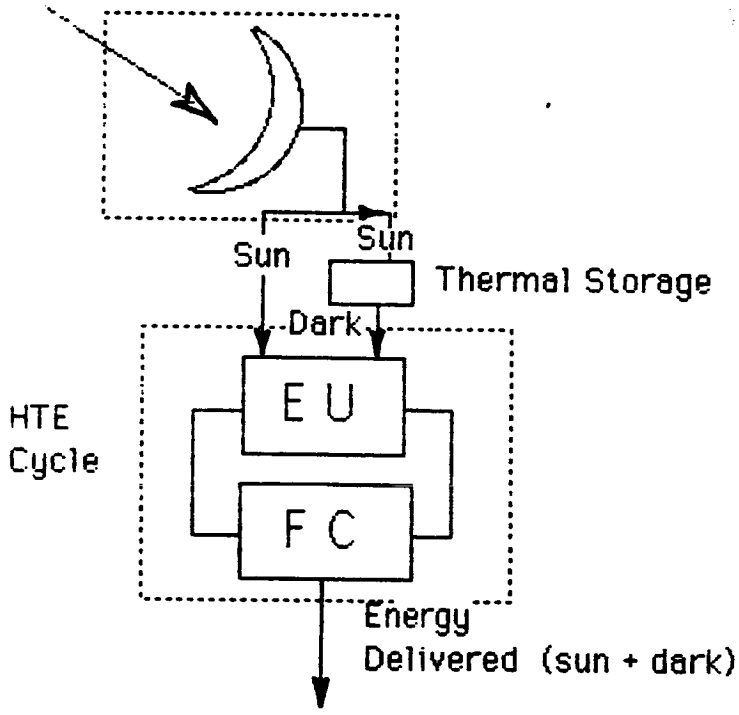
Sun
Sun
Thermal Storage
Dark
HTE
Cycle
E U
F C
Energy
Delivered (sun + dark)

Figure 6.

ELECTRICAL STORAGE OPTION

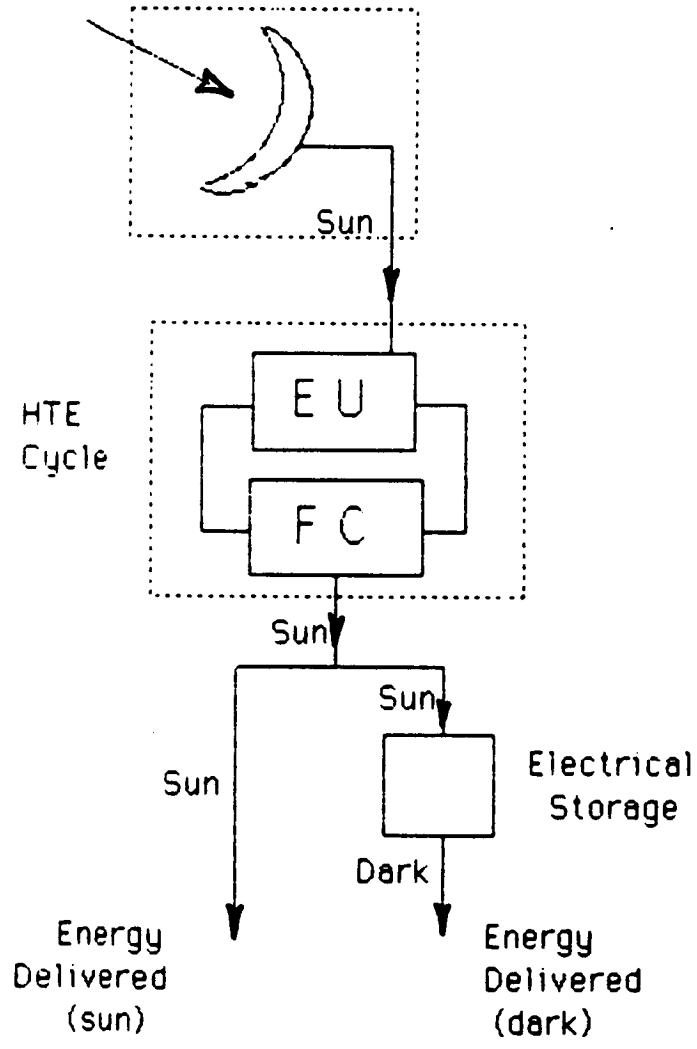

Figure 7.

Thus, even with 100 percent efficient electrical storage, the HTE cycle would have to be sized to produce 40.3 kWe.

Assuming 80 percent electrical energy storage efficiency, the HTE cycle is sized at 44.1 kWe, while the system efficiency (from Eq. 3) is 30.1 percent. The overall system efficiency is 21.1 percent and the needed collector area is $140.9 m^2$.

The input to the electrical storage system at 80 percent storage efficiency is 18.8 kWHR in order to provide the required 25 kWe dark period output. Since storage charging is done during the sun period, the rate of charging is 19.1 kWe.

3. Chemical Storage

The chemical storage concept involves operating the HTE cycle during the sun period to produce enough excess H_2 and O_2 to run the fuel cell during the dark period. Figure 8 presents the H_2 and O_2 storage configuration which illustrates the sun and dark period mass flow paths. The electrolyzer must produce at a rate (TD+TS)/TS greater than when operating continuously, so the HTE cycle devices must be sized at 1.61 times larger than the 25 kWe continuously operating cycle. Thus, a 40.3 kWe sized HTE cycle is required.

Assuming a fuel cell voltage efficiency of 95 percent, 4.6 kg of H_2O (or 0.5 kg Hz and 4.1 kg of O_2) must be stored. Thus, volume storage for 250 g moles of H_2, 125 g moles of O_2 and 4.6 liters of liquid water will be needed.

The storage efficiency for chemical storage is associated with the mechanical work done to store the H_2 and O_2. It is assumed that the storage work is done in isothermally compressing the H_2 and O_2 from 1 atmosphere to

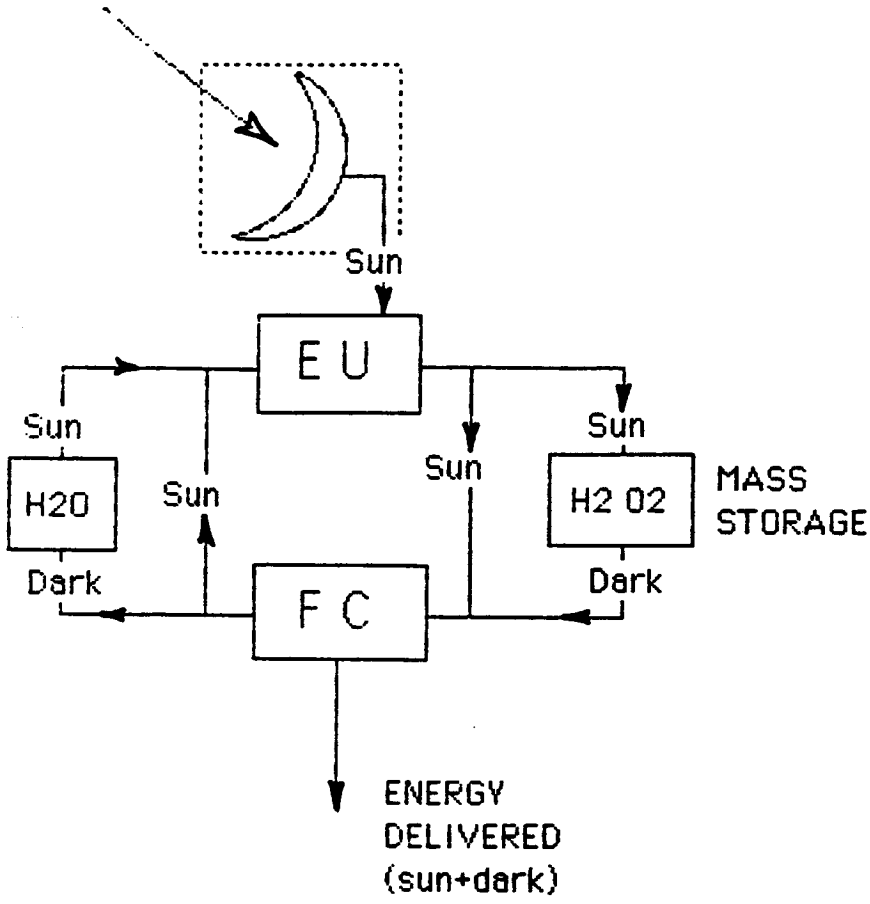
Sun
E U
Sun
Sun
Sun
H20
Sun
H2 02
MASS
STORAGE
Dark
Dark
F C
ENERGY
DELIVERED
(sun+dark)

Figure 8.

C-3

the storage pressure (Pstor):

$$Wstor = \frac{3}{2} R \cdot T \cdot \ln Pstor$$

A definition of storage efficiency, similar to previous options, must be derived from HTE cycle considerations, since this chemical option storage is integral to the cycle itself. The cyclic efficiency with chemical storage will be less than the "normal cycle" efficiency due to the work done to pressurize the electrolysis products for storage. Thus, the "integral storage cycle" efficiency ($\eta_{cyc\ stor}$) can be defined:

$$\eta_{cyc\ stor} = \frac{\text{Net work output per orbit}}{\text{Thermal input per orbit}}$$

$$= \frac{Pdel \cdot (TD + TS) - Nstor \cdot Wstor}{\frac{Pdel \cdot (TD+TS)}{\eta_{cyc}}}$$

where Nstor is the number of moles of water stored.

Noting that $\eta_{cyc\ stor}$ combines the previous definition of η_{cyc} and η_{stor}:

$$\eta_{cyc\ stor} = \eta_{cyc}\,\eta_{stor} = \eta_{cyc} \cdot \left(1 - \frac{Nstor \cdot Wstor}{Pdel \cdot (TD+TS)} \right)$$

So we now have a "standard" definition for this chemical storage efficiency:

$$\eta_{stor} = 1 - \frac{Nstor \cdot 3/2 \cdot RT \cdot \ln Pstor}{Pdel \cdot (TD + TS)}$$

Since Nstor = 250 g moles for the present situation:

$$\eta_{stor} = 1 - 0.00816 \ln Pstor,$$

Assuming a storage pressure of 20 atmospheres gives a 97.6 percent storage

efficiency, and the resulting combined cycle-storage system efficiency is 32.2 percent. This in turn leads to an overall system efficiency of 22.5 percent, requiring a collector area of 131.9m^2.

Summary of Storage Options

All three storage options possess individual attributes, such as reliability, weight, volume, etc., which are not addressed here. The actual selection of a storage option would have to take these and many more factors into consideration before an engineering selection could be made. It should also be noted that the time profile of the electrical load to be met will directly influence option performance via the storage required for a given profile.

However, with the conditions stated for the system options described, a summary comparison of the three options is presented in Table 2. The system efficiencies and resultant collector areas are seen to be very similar for the options, but the HTE cycle size which must be installed is much less for the thermal storage option. Thus, thermal storage was chosen as the option to be used with the system parametric studies below.

TABLE 2. STORAGE OPTION COMPARISON

	THERMAL ENERGY	CHEMICAL ENERGY	ELECTRICAL ENERGY
STORAGE EFFICIENCY(%)	90	97.6	80
HTE CYCLE SIZE (KWe2)	25	40.3	44.1
OVERALL SYSTEM EFFCIENCY (%)	22.2	22.5	21.1
COLLECTOR AREA (m2)	133.9	131.9	140.9

PARAMETRIC ANALYSES

The parametric analyses are structured to provide results for two separate purposes: the determination of optimium operating conditions, and the investigation of system sensitivities to parametric variations around the optimum conditions. The optimizations and sensitivities are done for both current and future technology devices, with different combinations of the devices used to examine the effect of developing a particular device.

Important Parametric Variables

In addition to defining the technology values and establishing the system configuration, it is necessary to identify the major variables important to system operation. These variables can be identified by looking at the cycle efficiency equation,

$$\eta_{cyc} = \frac{Wf - We}{Qhot} = \frac{\eta_{fc} \cdot \Delta Gf - \Delta Ge/\eta_e}{\Delta He - (\Delta Ge/\eta_e) + Qhx}$$

and by substituting using many relations which are defined and described in the subsection below:

$$\eta_{cyc} = \frac{Vf \cdot \eta_{cf} \cdot n \cdot F - Ve \cdot n \cdot F/\eta_{ce}}{\Delta He - Ve \cdot n \cdot F/\eta_{ce} + (1 - \varepsilon hx)(h_{Th} - h_{Tc})}$$

It is seen that two major variable types influence the cycle efficiency: device voltage (Vf, Ve) and device current efficiency (η_{cf}, η_{ce}). These variables are the one expected to be of importance, and both voltage and current efficiency are known to be functions of the device operating current density. As is shown below, the optimizations and sensitivities were performed against these identified important variables.

Optimization Scheme

The generalized function to be optimized is assumed to be related to the fuel cell and electroylzer areas in the additive manner:

$$BT = BF \cdot AF + BE \cdot AE \ , \qquad (4)$$

where BT represents the total system parameter (mass, volume, area, cost, etc.), BF and BE represent parametric values (or functions) on a unit area basis, and AF and AE represent the fuel cell and electrolyzer cell areas, respectively.

The optimization of the generalized function is performed assuming that the system is operating with a given net power (Pnet) and with given fuel cell and electrolyzer operating curves (V versus J). The areas to be used depend on the current density, and resulting device efficiency, desired for the overall system. Thus, the three variables chosen as independent are:

$\dot{N}$ - The molal fuel flow rate which determines the overall current developed and used

JF - The fuel cell current density: $JF = \frac{If}{AF}$

JE - The electrolyzer current density: $JE = \frac{Ie}{AE}$

Now writing the generalized function, Eq. 4, in terms of the three variables,

$$BT = \frac{BF \cdot If}{JF} + \frac{BE \cdot Ie}{JE}$$

where $If = Io \cdot \eta cf$ and $Ie = \frac{Io}{\eta ce}$

with $Io = n \cdot F \cdot \dot{N}$, n = #electrons per reaction

F = Faraday's constant

and cf and ce are the current efficiences for the fuel cell and electrolyzer, respectively. So, the area function becomes,

$$BT = \frac{BF \cdot n \cdot F \cdot \eta cf \cdot \dot{N}}{Jf} + \frac{BE \cdot n \cdot F \cdot \dot{N}}{\eta ce \cdot Je} = f(JF, JE, \dot{N})$$

and defining $C1 = n \cdot F \cdot \eta cf$ and $C2 = \frac{n \cdot F}{\eta ce}$

$$\text{then, } BT = \frac{BF \cdot C1 \cdot \dot{N}}{JF} + \frac{BE \cdot C2 \cdot \dot{N}}{JE} \qquad (5)$$

where it is assumed current efficiency (ηcf, ηce) is a constant for the conditions given.

A constraining relation can be defined for the given net power level,

$$Pnet = Pf - Pe$$
$$= If \cdot Vf - Ie \cdot Ve$$

where the Vf and Ve are the operating voltages for the fuel cell and electrolyzer, both of which are functions of their respective current densities. Substituting for the currents as before:

$$Pnet = n \cdot F \cdot \eta cf \cdot \dot{N} \cdot Vf - \frac{n \cdot F \cdot \dot{N} \cdot Ve}{\eta ce}$$
$$= C1 \cdot \dot{N} \cdot Vf - C2 \cdot \dot{N} \cdot Ve$$

So, the constraint relation can be written:

$$(JF, JE, \dot{N}) = Pnet - C1 \cdot \dot{N} \cdot Vf + C2 \cdot \dot{N} \cdot Ve = 0 \qquad (6)$$

where $Vf = f(JF)$ and $Ve = f(JE)$.

Extremum by Lagrangan Multiplier

The extremum of the BT function, Eq. 5, may now be found subject to the constraint, Eq. 8, by using the Lagrangan multiplier approach. This approach yields four equations and four unknowns (JF, JE, $\dot{N}$, λ) with three equations arising from the external condition,

$$\frac{\partial F}{\partial Xi} - \lambda \frac{\partial \phi}{\partial Xi} = 0 \qquad i = 1, 2, 3 \qquad Xi = (JF, JE, \dot{N}) \tag{7}$$

and the constraint equation itself,

$$\phi = 0 .$$

Substituting into the three extremal condition equations, Eq. 9, yields:

$$\frac{BF}{JF^2} - \lambda \frac{\partial Vf}{\partial JF} = 0$$

$$\frac{BE}{JE^2} + \lambda \frac{\partial Ve}{\partial JE} = 0$$

$$\frac{Bf \cdot C1}{JF} + \frac{BE \cdot C2}{JE} - \lambda(-C1 \cdot Vf + C2 \cdot Ve) = 0$$

and the constraint equation, Eq. 6, provides the fourth equation for the four unknowns:

$$Pnet - (C1 \cdot Vf + C2 \cdot Ve) \cdot \dot{N} = 0$$

Thus, the mathematical problem is to solve four non-linear equations for the four variables. Note that the Vf and Ve functions must be inserted into these equations before solving. Also note that if the BF and BE terms are

functions of area, the areas would have to be converted to N and J functions as outlined earlier.

Unconstrained Optimization Approach

It should also be noted that the optimization problem could be solved as an unconstrained problem by combining the generalized function and the constraint equation by eliminating a variable through substitution. This leaves the following expression in two variables to be optimized:

$$BT(JF, JE) = \frac{Pnet}{C1 \cdot VF - C2 \cdot VE}\left(\frac{BF \cdot C1}{JF} + \frac{BE \cdot C2}{JE}\right)$$

where VF, VE, BF and BE are known explicit functions in JF and JE.

Specific Solutions: Linear Polarization Curves

Both the non-linear equation approach and the unconstrained optimization approach were used by application of an algorithm described in [ref. 21]. However, for the case where the voltage-current density polarization curves can be described by linear relations of the form:

$$Vf = Vfo - a \cdot JF$$

$$Ve = Veo + b \cdot JE,$$

then the Lagrangian method yields the exact solution:

$$JF = \frac{C1 \cdot Vfo - C2 \cdot Veo}{2 \cdot C1 \cdot a + 2 \cdot C1 \cdot (a \cdot b \cdot BE/BF)^{1/2}}$$

$$JE = \frac{C1 \cdot Vfo - C2 \cdot Veo}{2 \cdot C1 \cdot (a \cdot b \cdot BF/BE)^{1/2} + 2 \cdot C2 \cdot b}$$

with $\dot{N}$ given by substitution back into Eq. 8. This approach using linear

polarization curves was utilized in this investigation in order to accommodate the large number of parametric variations investigated.

Example Results

The optimization of the HTE cycle to minimize mass, volume, and/or cell area was performed using the exact linearized procedure. The HTE cycles examined were grouped into three areas:

- Current Technology - cycle composed of current fuel cell (alkaline) and a current solid oxide cell electrolyzer operating at 1000°C;
- Near Term Technology - three cycles composed of:
  a. Current fuel cell and solid oxide electrolyzer at 1500°K,
  b. Advanced fuel cell (SPE-type) and current solid oxide electrolyzer at 1000°C,
  c. Advanced fuel cell and solid oxide electrolyzer at 1500°K; and
- Future Technology - cycle composed of future fuel cell and solid oxide electrolyzer operating at 1800°K.

The characteristics of these devices are described in Table 1 and Figure 4. The results discussed below were generated assuming a 1 kWe cycle output.

The generalized system parameter, BT, was optimized for a range of fuel cell to electrolyzer parametric ratios (BF/BE) for the three basic technology cases. The results of these optimizations is presented graphically in Figure

9. Also shown in Figure 9 is the effect of device current efficiency on the value of BT. Note that the current efficiency variation causes a large variation in the system parameter, especially for the current technology case.

More detail illustrating this system sensitivity to current density efficiency is presented in Figure 10. The minimum total cell area for the HTE cycle is shown as a function of the fuel cell current efficiency and the electrolyzer current efficiency for a current technology system.

In the analysis of 'off-optimum' operating conditions, the 'brute force' method described earlier was used to generate a range of operating conditions. Figure 11 presents an example of this approach using current technology devices. The variation around the minimium total area can be seen, as well as the individual fuel cell and electrolyzer areas. Figure 12 presents another aspect of data from these same 'brute force' simulation runs. It is seen that the electrolyzer operating point is relatively constant, no mattery at what condition the fuel cell is operating.

Figure 9.

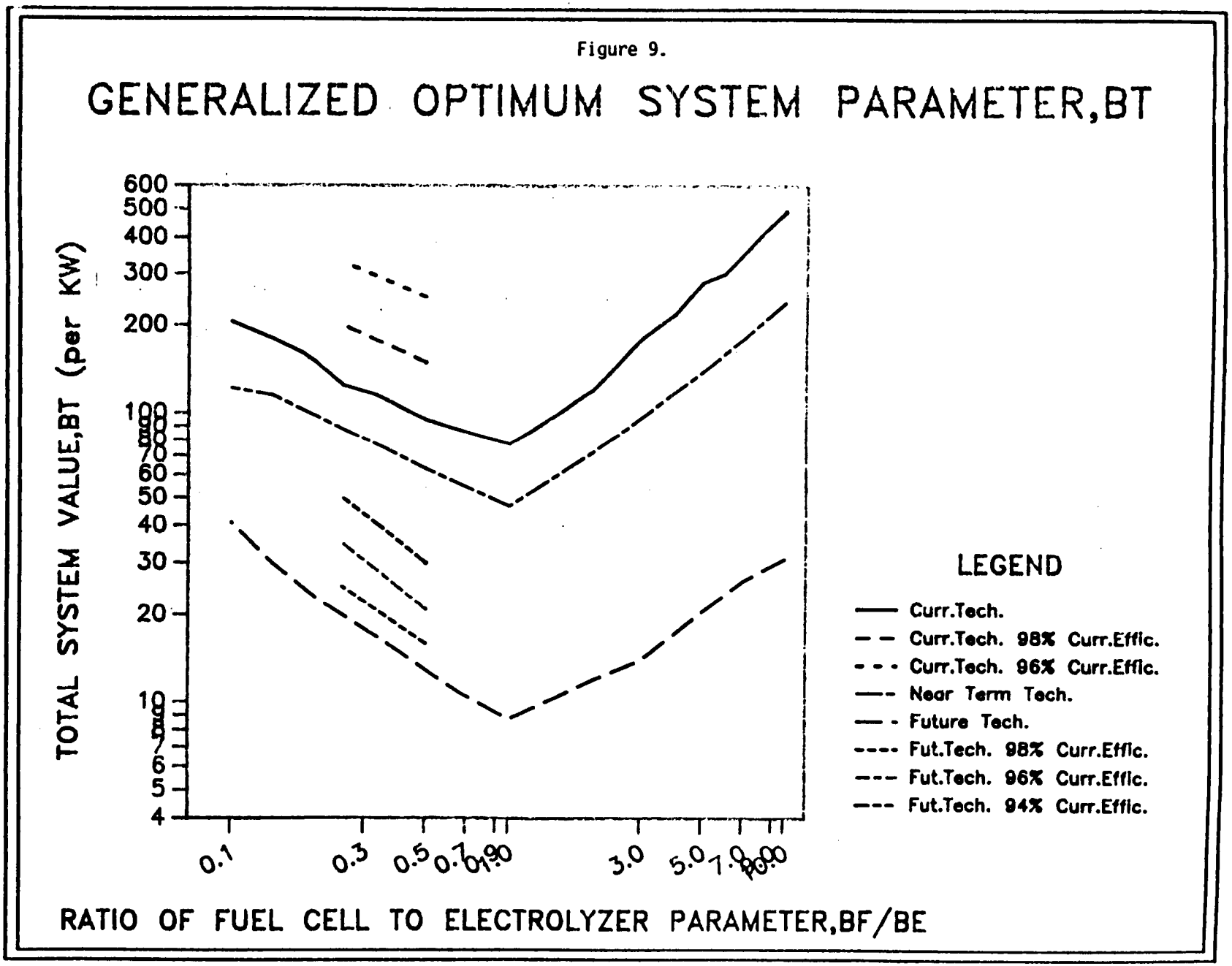
GENERALIZED OPTIMUM SYSTEM PARAMETER,BT
TOTAL SYSTEM VALUE,BT (per KW)
600
500
400
300
200
100
60
50
40
30
20
10
6
5
4
0.1
0.3
0.5
0.7
1.0
3.0
5.0
10.0
RATIO OF FUEL CELL TO ELECTROLYZER PARAMETER,BF/BE
LEGEND
Curr.Tech.
Curr.Tech. 98% Curr.Effic.
Curr.Tech. 96% Curr.Effic.
Near Term Tech.
Future Tech.
Fut.Tech. 98% Curr.Effic.
Fut.Tech. 96% Curr.Effic.
Fut.Tech. 94% Curr.Effic.

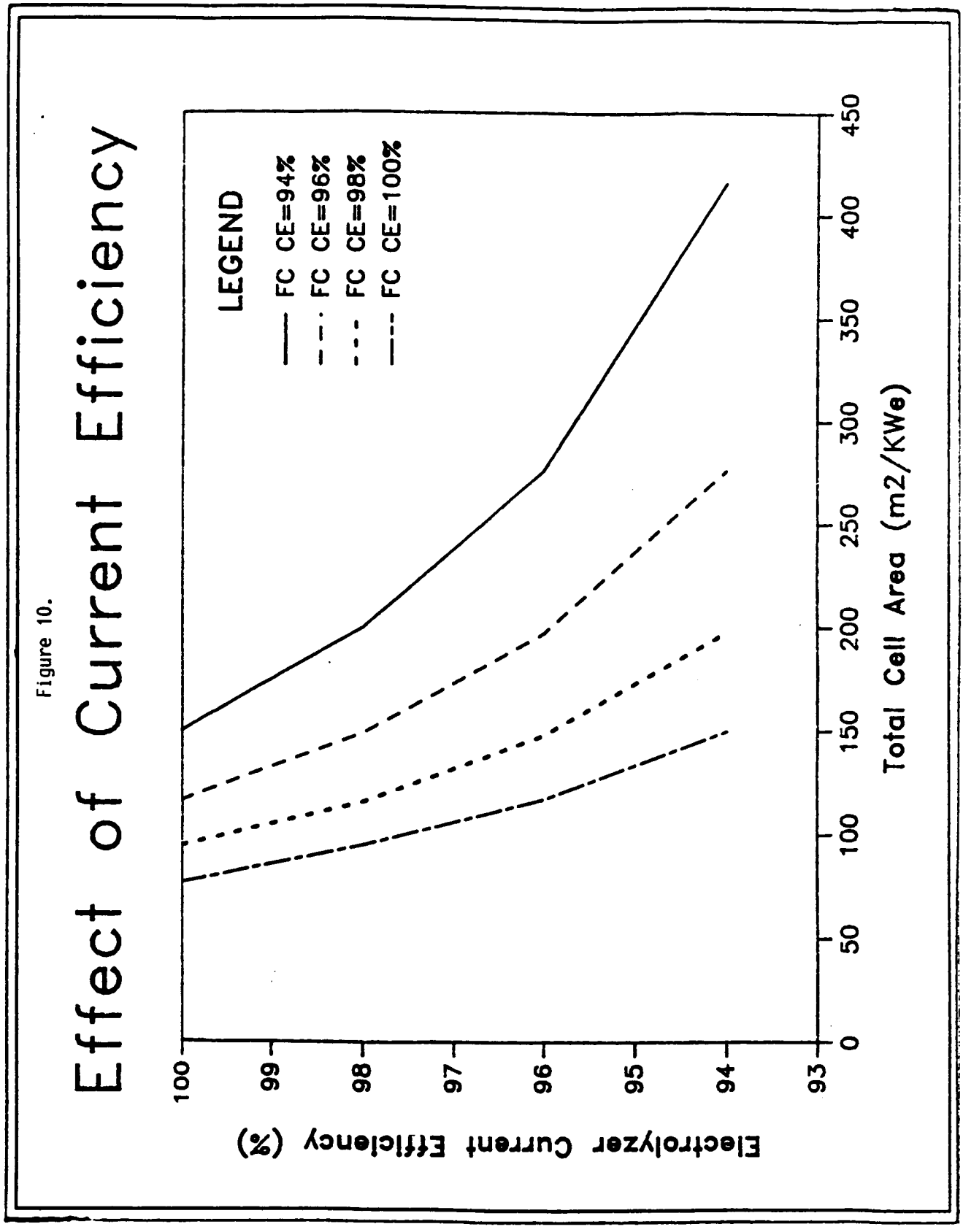
Effect of Current Efficiency
LEGEND
FC CE=94%
FC CE=96%
FC CE=98%
FC CE=100%
Electrolyzer Current Efficiency (%)
100
99
98
97
96
95
94
93
0
50
100
150
200
250
300
350
400
450
Total Cell Area (m2/KWe)

Figure 10.

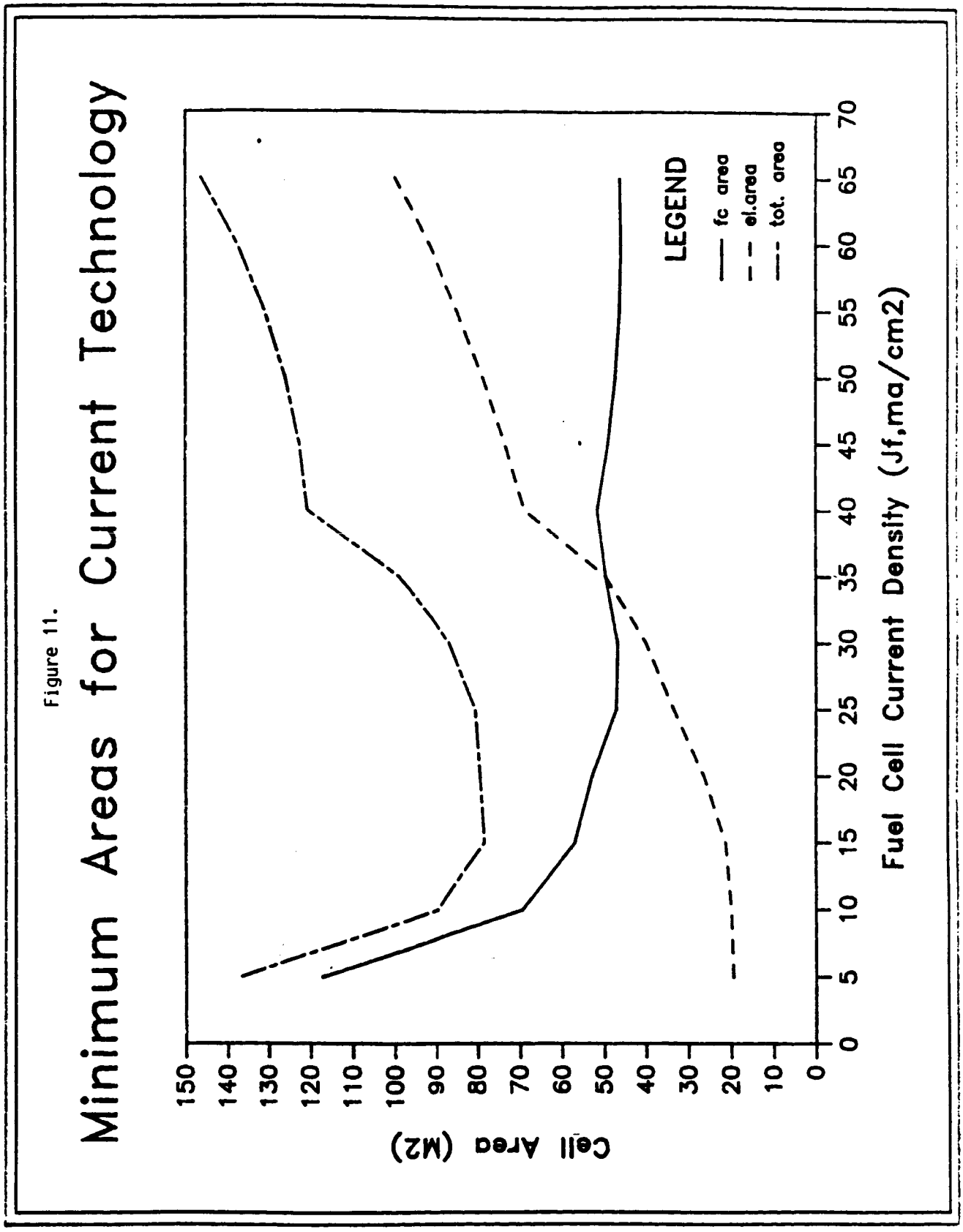
Minimum Areas for Current Technology
Cell Area (M2)
Fuel Cell Current Density (Jf,ma/cm2)
LEGEND
fc area
el.area
tot. area
150
140
130
120
110
100
90
80
70
60
50
40
30
20
10
0
0
5
10
15
20
25
30
35
40
45
50
55
60
65
70

Figure 11.

Figure 12.

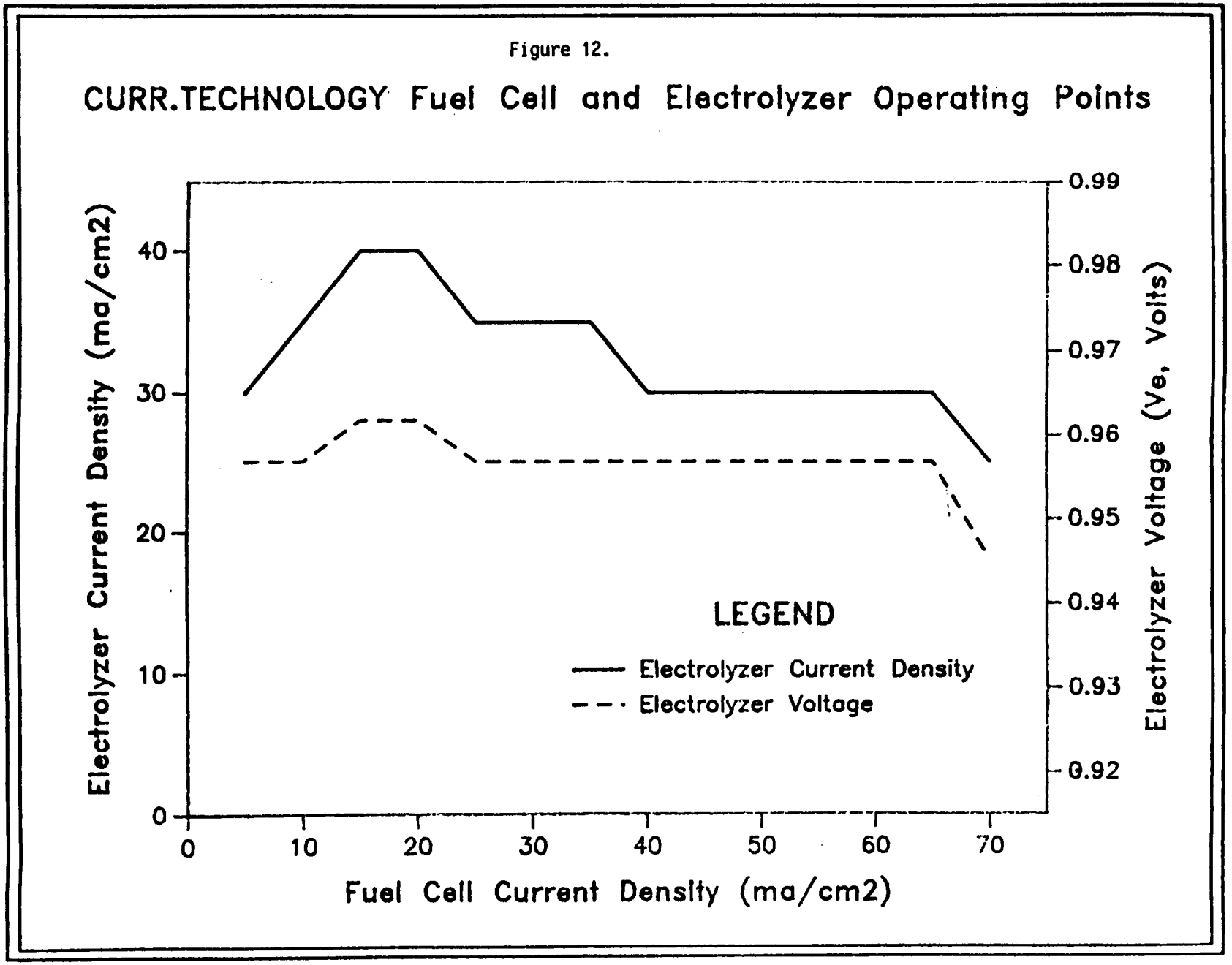
CURR.TECHNOLOGY Fuel Cell and Electrolyzer Operating Points
Electrolyzer Current Density (ma/cm2)
Electrolyzer Voltage (Ve, Volts)
Fuel Cell Current Density (ma/cm2)
0
10
20
30
40
50
60
70
0.92
0.93
0.94
0.95
0.96
0.97
0.98
0.99
LEGEND
Electrolyzer Current Density
Electrolyzer Voltage

Table 3.

SUMMARY OF SYSTEM DESIGN PARAMETERS

	1 KWe MODULE				
	CYCLE EFFIC.[1] (%)	TOTAL CELL AREA [2] (m2)	TOTAL VOLUME (m3)	TOTAL MASS (kg)	GROSS POWER (KW)
CURRENT TECH. (98% curr.effic.)	26.8	116.2	1.85	1606.5	11.8/10.8
NEAR-TERM TECH. (98% curr.effic.)					
a)Curr.FC/1500K EU	30.8	66.9	0.85	506.7	8.6/7.6
b)Fut.FC/Curr. EU	31.5	31.7	0.37	482	11.0/10.0
c)Fut.FC/1500K EU	35.8	19.8	0.2	89.2	8.3/7.3
FUTURE TECH. (99% Curr.Effic.)	43.4	9.6	0.1	43.3	5.8/4.8

[1] 95% Heat Exchanger Effectiveness
[2] Optimized Parameter

Figure 13.

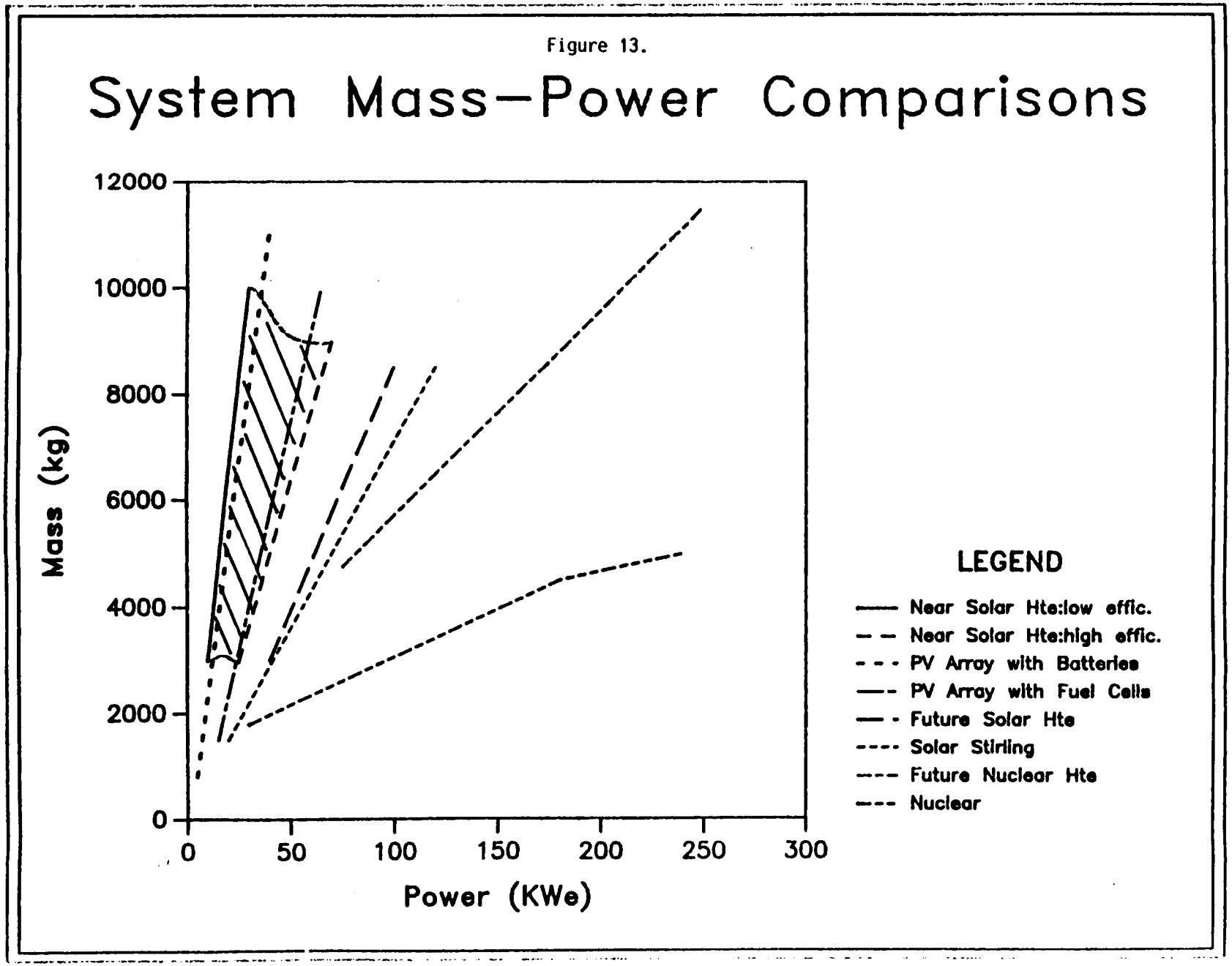
System Mass–Power Comparisons
12000
10000
8000
6000
4000
2000
0
Mass (kg)
0
50
100
150
200
250
300
Power (KWe)
LEGEND
Near Solar Hte:low effic.
Near Solar Hte:high effic.
PV Array with Batteries
PV Array with Fuel Cells
Future Solar Hte
Solar Stirling
Future Nuclear Hte
Nuclear

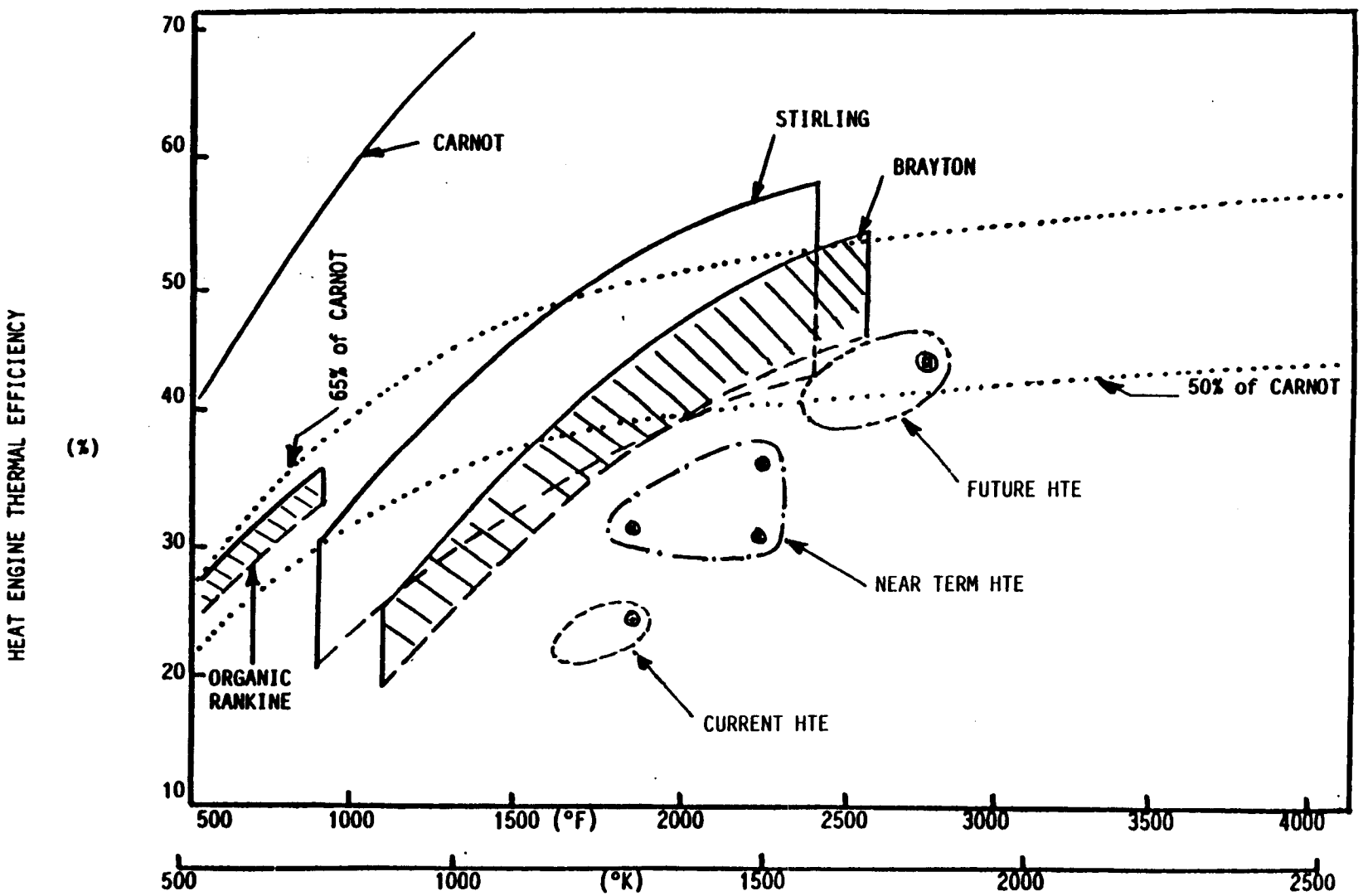

Figure 14 . THERMODYNAMIC CYCLE COMPARISONS FOR VARIOUS OPERATING TEMPERATURES

SUMMARY

The HTE cycle was examined using simulations which identified optimum system operating conditions under various parametric situations (i.e., minimum cell area, volume, mass, etc.). These optimum conditions were found for systems composed of fuel cell and electrolyzer technology representing current, near term, and future developmental efforts. A summary of general HTE cycle design parameters, fuel cell and electrolyzer devices only, is presented in Table 3 and is based on an area minimization.

The Table 3 data represents a 1 kWe module, and it can be seen that while current technology HTE cycles could be constructed with reasonable efficiencies, the mass, volume, and cell areas needed are extremely large. Near term developments would lead to significant mass, area, and volume reductions, while future technology developments will also provide significant increases in cycle efficiency and device sizing requirements (gross power).

Comparison to Other Cycles

The data presented in Table 3 allows a comparison between the HTE cycle and other power cycles. A comparison of overall system mass-to-power ratios is presented in Figure 13. The graph itself is adapted from [Ref. 2], with the entire system mass being included for each system type, including the HTE cycles with solar collectors and radiators [Ref. 9]. The current technolgy HTE curve is almost coincident with the left axis, but near term technology HTE's are in the cross-hatched area along with PV systems. Future technolgy HTE's are shown as similar to the best solar dynamic, and even approaching

nuclear dynamic systems.

Another comparison can be made in terms of efficiency and operating temperature. In Figure 14, various dynamic systems are represented, with the HTE cycles presented by time of technology development. It should be noted that while the HTE cycle appears to be 'under' the curves of the Brayton and Stirling cycles, it can be thought of as being to the 'side' of them, meaning the HTE operates at higher temperature. This type of interpretation is possible when it is realized that the HTE cycle does not have reciprocating or revolving mechanical parts which operate at these high temperatures.

Further Developments

Fuel cells and the electrolyzer exist to build a HTE today. However, it would be large, heavy and costly. The cycle efficiency is reasonable, but it was found that the current technology cycle is very sensitive to device current efficiency. Two and three percent current efficiency losses correspond to doubling and tripling the cell areas needed. Thus, a current technology HTE cycle would represent a formidable engineering challenge.

In the near term, the fuel cell and/or the electrolyzer can be improved. The solid oxide electrolyzer existing today might be able to be modified to work at 1500°K, but it would probably take a major developmental effort to gain the fuel cell improvements described in Figure 4 and Table 1. It appears reasonable that a near term HTE, as represented on Figures 13 and 14, could be demonstrated with two to five years of development. Such a HTE system would exhibit comparable mass and efficiency to current PV and solar dynamic systems.

The future HTE systems are envisioned as operating at 1800°K electrolyzer heat input, with an advanced SPE-type fuel cell at 100°C (373°K). Both the electrolyzer and fuel cell will require major developmental efforts to achieve the desired performance. However, a HTE power cycle operating at these conditions will be as-good-as or better than other envisioned solar cycles, while still retaining its 'no moving parts' attraction.

REFERENCES

1. "Conceptual Design and Evaluation of Selected Space Station Concepts," JSC-19521, NASA/Johnson Space Center, 1983.

2. Buden, et al; 19th IECEC Proceedings, Vol. I, p. 89. San Francisco, CA, 1984.

3. Liebhafsky, H. A., "The Fuel Cell and the Carnot Cycle," Journal of the Electrochemical Society, Vol. 106, pp. 1068-1071, 1959.

4. de Bethune, A. J., "Fuel Cell Thermodynamics," Journal of the Electrochemical Society, Vol. 107, pp. 937-939, 1960.

5. Abraham, B. M. and Schreiner, F., "General Principles Underlying Chemical Cycles Which Thermally Decompose Water into the Elements," Industrial and Engineering Chemistry, Fundamentals, Vol. 13, No. 4, pp. 305-310, 1974.

6. Veziroglu, T. N. and Kakac, S., "Solar Hydrogen Energy System and Solar Hydrogen Production Methods," International Symposium-Workshop on Solar Energy, Cairo, Egypt, pp. 275-296, June 1978.

7. Liepa, M. A. and Borhan, A., "High Temerature Steam Electrolyses: Technical and Economic Evaluation of Alternative Process Designs", International Journal of Hydrogen Energy, Vol. II, No. 7, pp. 435-442, 1986.

8. Chum, H. L. and Osteryoung, R. A., "Review of Thermally Regenerative Electrochemical Systems", SERI/TR-332-416, Solar Energy Research Institute, Golden, CO, August 1980.

9. "Space Station Electrical Power System Configuration Impact Assessment," JSC-19994 Power System Branch, NASA/Johnson Space Center, August 1984.

10. Morehouse, J. H., "Thermally Regenerative Hydrogen/Oxygen Fuel Cell Power Cycles", Final Report NASA/ASEE Summer Faculty Program, NASA/JSC; Houston, TX, August 1985.

11. Morehouse, J. H., "Thermally Regenerative Hydrogen/Oxygen Fuel Cell Power Cycles", Solar Engineering - 1986: Proceedings of the ASME Solar Energy Conference, Anaheim, CA, pp. 113-119, April, 1986.

12. Isenberg, A. O., "Cell Performance and Life Characteristics of Solid Oxide Electrolyte Fuel Cells," Proceedings of the Conference on High Temperature Solid Oxide Electrolytes Brookhaven National Lab; Vol. I, pp. 5-15, October 1983.

13. Masalick, N. J., et. al., "Hydrogen Production Employing High-Temperature Solid Oxide Cells," Proceedings of the 19th IECEC, San Francisco, CA, pp. 1415-1420, 1984.

14. Powell, J. R. and Fillo, J. "Advanced Synfuel Production with Fusion," Proceedings of the 14th IECEC, Boston, MA, pp. 1549-1552, 1979.

15. Fee, D. C., et. al., "Solid-Oxide Fuel Cell Performance," 2nd Solid Oxide Fuel Cell Workshop, Brookhaven National Lab, August 1983.

16. Doenitz, W., et. al., "High Temperature Electrolysis of Water Vapor - Status and Perspectives of the German Research and Development Activities," Proceedings of the Conference on High Temperature Solid Oxide Electrolytes, BrookHaven Nat. Lab (BNL51728), pp. 67-80, 1983.

17. Dietrich, G. and Shaffer, W. "Advances in the Development of Thin-Film Cells for High Temperature Electrolysis, International Journal of Hydrogen Energy, Vol. 9, No. 9, pp. 747-752, 1984.

18. Personal Communication - Power Branch, NASA/JSC, Houston, Texas, August 1986.

19. Personal Communication - Venture Technology Group, Westinghouse R&D Center, Pittsburg, PA, July 1986.

20. "Regenerative Fuel Cells: Space Station Design Definition", Life Systems, Inc. Technical Status Report, TR-862-6A, November 1985.

21. Dennis, J. E. and Schnabel, R. B., "Numerical Methods for Unconstrained Optimization and Nonlinear Equations", ISBN 0-13-627216-9, Prentice-Hall, 1983.